A Comparison of Imaging Spectrometers

Charles L. Bennett

L-43, Lawrence Livermore National Laboratory, P.O. Box 808, Livermore, California, 94550

Abstract. Realistic signal to noise performance estimates for the various types of instruments being considered for NGST are compared, based on the point source detection values quoted in the available ISIM final reports. The corresponding sensitivity of the various types of spectrometers operating in a full field imaging mode, for both emission line objects and broad spectral distribution objects, is computed and displayed. For the purpose of seeing the earliest galaxies, or the faintest possible emission line sources, the imaging Fourier transform spectrometer emerges superior to all others, by orders of magnitude in speed.

1. Introduction

The Next Generation Space Telescope (NGST), if successful, will represent a tremendous advance in several dimensions. For a relatively small investment, great strides in our understanding of the universe will be made. One of the most important early decisions, and one that will determine the quality of the legacy of NGST, is the constitution of the science instruments that will be on board. A key question relates to the utility of imaging spectrometers. An imaging spectrometer is almost never as sensitive as a non-imaging spectrometer for a single "point" source. However, for observations over a wide field of view containing many point sources, or for observations of fields of view containing spatially distributed sources, the spatial multiplexing characteristics of imaging spectrometers must be carefully traded against point source sensitivity.

There has been much discussion of the relative performance, and the scientific utility, of the various types of imagers and spectrometers that might be flown on NGST. In particular, the final reports from a number of year long ISIM (Integrated Science Instrument Module) studies have recently become available.[1] These studies represent the currently best available starting point for a comparison between the variety of approaches to the design of imagers and spectrometers for NGST.

---

[1] See the web site:
http://www.mipd.gsfc.nasa.gov/isim/science.htm/, for the currently available ISIM final reports. Another useful web site reference is: http://ngst.gsfc.nasa.gov/public_docs_date.html/, which maintains an up to date, chronologically ordered list of publicly available documents relevant to NGST.
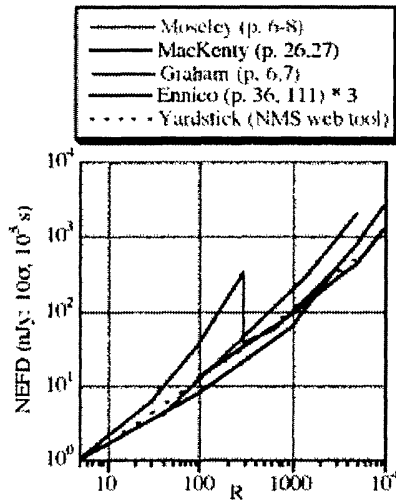
Figure 1. The Noise Equivalent Flux Density (NEFD), for point source detection in K band, in a 10^5 s exposure, at the 10 σ level of statistical confidence is plotted as a function of spectral resolution R for the various ISIM point design instruments. The solid curves are identified by the first author on the ISIM final reports, and the page numbers from which the point source sensitivity estimates were taken. The Ennico values have been multiplied by a factor of 3, to reflect a 3 × 3 greater sampling for point sources than was used in their report. The dashed line represents the point source sensitivity estimates for the NGST yardstick design based on the NGST Mission Simulator (NMS), which is located at the web site: http://www.ngst.stsci.edu/nms/main/index.html/.

In view of the wide range in approaches, the point source sensitivity, as a function of spectral resolution, is remarkably consistent between the various ISIM designs, as can be seen for the K band in figure 1 and for 10 μm observations in figure 2. The numbers plotted in these two figures have been scaled, where necessary, to correspond to a total exposure time of 10^5 s, with neglect of overhead time, and to a statistical significance of 10 σ. It is important to note that the degree of spatial multiplexing varies greatly between and among the various curves plotted. In particular, the discontinuity that appears in the Graham curves in both figures 1 and 2, at $R = 300$ and $R = 100$ respectively, corresponds to a transition in the Graham point design from a full field Imaging Fourier Transform Spectrometer (IFTS) to a dispersed mode IFTS, which is a form of Multi Object Spectrometer (MOS).

If only single point sources were to be observed by NGST, then the point source sensitivity would be an appropriate performance metric for comparison of the various instrumental configurations. However, most of the components of the NGST Design Reference Mission (DRM), either explicitly involve observations of large numbers of extended objects, e.g. the galaxy DRM, or could benefit by the acquisition of large numbers of objects. The point source sensitivity, therefore, does not by itself determine the relative instrumental sensitivity for
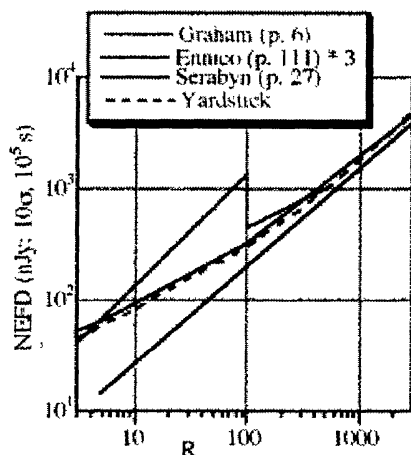
Figure 2.   The Noise Equivalent Flux Density (NEFD), for a 10 μm point source detection in a 10^5 s exposure, at the 10 σ level of statistical confidence is plotted as a function of spectral resolution R for the various ISIM point design instruments. The annotation of the curves is similar to that of figure 1.
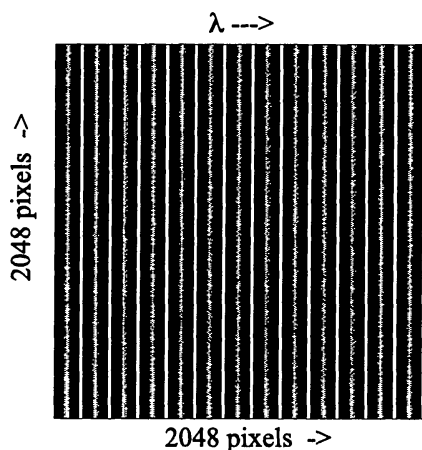

Figure 3.   A schematic mapping dispersive spectrometer.

execution of the DRM. It is necessary to include the spatial multiplexing factor in order to properly compare the various alternatives.

2.   Imaging Spectrometers

In the Ennico report (pp. 37–40), it is shown how a dispersive spectrometer, (DS), may be used as a full field imaging spectrometer. In this approach, a set of parallel slits are placed in an object plane in such a way that nearly every pixel in the image plane is utilized. A schematic representation of this arrangement is shown in figure 3, where the color is indicative of the wavelength of light that would fall at a given position in the image plane. Very efficient use of pixels in
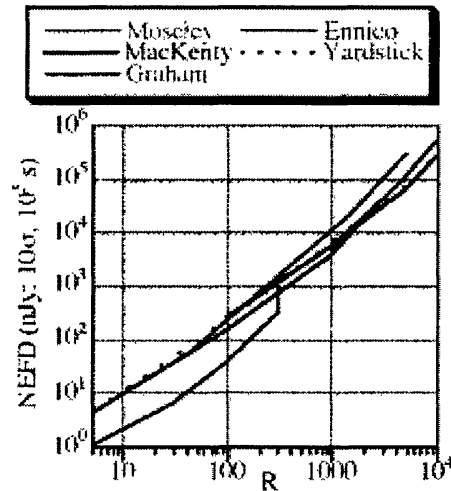
Figure 4.   The NEFD sensitivity to point sources scaled from the values in figure 1 by assuming that full field imaging spectroscopy is acquired.

the FPA detector may be made in this way, as the "red" edge corresponding to a given slit may be placed very near the "blue" edge of an adjacent slit, without fear of confusion.

The number of pixels, M, needed along the dispersion direction is determined by the spectral resolution, and the spectral bandpass coverage. In order for such a mapping dispersive spectrometer to acquire full field imaging spectroscopy, the minimum number of separate pointings of the line of sight required is M. Obviously, the time available to each of the separate pointings is down by a factor of M from that available for the full image set. The relation between the number of pixels needed in the dispersion direction depends only slightly on the type of DS. A good estimate, based on a grating spectrometer case, is obtained by assuming that a single grating setting obtains a single octave of spectral coverage. In this case $M = 1.33 * R_{\text{average}}$. In order to cover the full 0.6–5 μm NIR range, three grating settings are needed.

In figure 4, the point source sensitivities of figure 1 from the various ISIM final reports have been converted to the sensitivities for full field imaging spectroscopy by assuming that the total number of separate exposures for the DS is given by $4 * R$. In this case, the IFTS has a clear sensitivity advantage for full field imaging spectroscopy. It should be noted that the IFTS sensitivity calculations are dependent on the shape of the spectral energy distribution, in contrast to the case of a DS. It turns out that the IFTS sensitivity to emission line sources is very much greater than for continuum sources. This is shown in figure 5, where a comparison of the IFTS sensitivity to that of the yardstick for imaging spectroscopy is displayed. At a resolution of $R = 5000$, the IFTS has a speed advantage of more than two orders of magnitude with respect to the yardstick NGST ISIM. This enormous speed advantage implies that some types of observations, e.g. spatially resolved kinematics of high z objects, become practical that would not previously have been thought possible. The great sensitivity of an IFTS to emission lines is particularly important in the NGST context, since the high spectral resolution components of the DRM are domi-
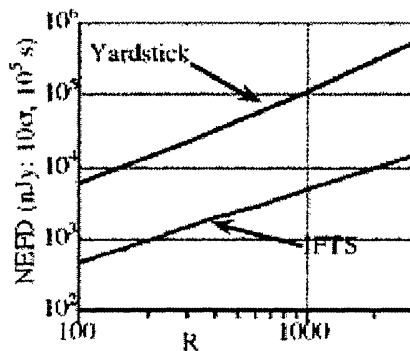
Figure 5.   The K band NEFD sensitivity to point source emission lines for the NGST yardstick design operating in mapping mode is compared to that of an imaging Fourier transform spectrometer.

Figure 6.   The 10 μm NEFD sensitivity to point source emission lines for the NGST yardstick design operating in mapping mode is compared to that of an imaging Fourier transform spectrometer. In this case the spectral bandpass acceptance of the IFTS is 20%.
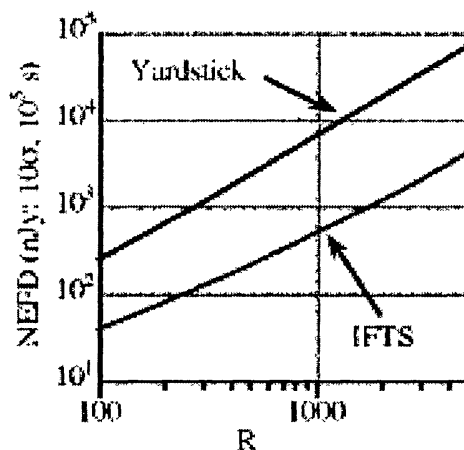
nated by emission line spectroscopy. Also, since the IFTS obtains a spectrum for every pixel, there is no sacrifice in the quality of the imaging associated with the acquisition of high spectral resolution data, as tends to be the case with mapping dispersive spectrometers.

A similar comparison for the MIR band is shown in figure 6 between the sensitivity of the yardstick ISIM in mapping mode and an IFTS with a bandpass filter spanning a 20% bandpass at 10 μm. Since the zodiacal emission increases so rapidly with wavelength beyond 5 μm, it is necessary for the IFTS to operate with bandpass limiting, cold stopped filters in place, in order to obtain reasonable sensitivity levels at the short wavelength end of any given spectral interval.
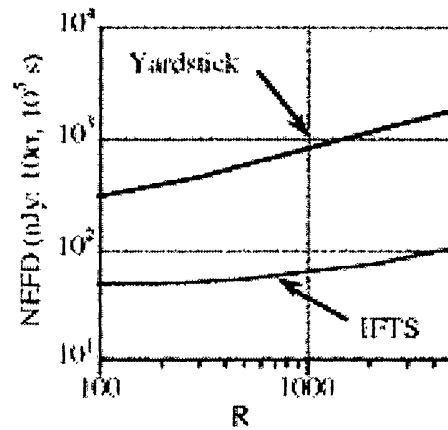
Figure 7. The K band NEFD continuum level associated with sources detected by emission lines for the NGST yardstick design in mapping mode is compared to that of an imaging Fourier transform spectrometer.

In the case of emission lines spectra, once again the IFTS emerges with a great sensitivity advantage over a mapping dispersive spectrometer.

The level of the continuum flux relative to the intensity of an emission line depends on the equivalent width of the emission line, and the spectral resolution R. Until an emission line is resolved, the observed peak intensity grows in proportion to R. Since the point source detection thresholds for all of the proposed instruments for NGST also tend to rise linearly with R, the continuum level associated with the detection threshold for emission lines tends to be approximately independent of spectral resolution. As an example, the continuum levels associated with the 10 σ detection of Lyα lines red shifted to K band, that have a rest frame equivalent width of 10 Å is shown in figure 7 for both the NGST yardstick ISIM and the IFTS. The slight rise in the IFTS curve at the highest resolution results from the gradually increasing contribution of detector read noise. In contrast, the monotonically rising curve for the yardstick ISIM curve results from the much greater sensitivity of the yardstick ISIM to the detector dark current.

The IFTS sensitivity levels that may be obtained are staggering. At a resolution $R = 5000$, sufficient to clearly separate the [OII] doublet, or the [OIII], Hβ complex, the IFTS sensitivity in a single deep 10^5 s exposure reaches an AB magnitude of 26 in K band for each and every object located within the full field of view of $5.3' \times 5.3'$. This sensitivity advantage for faint emission line objects is an intrinsic strength of the imaging Fourier transform approach to imaging spectroscopy. In the last section of this report, from analytic expressions for the sensitivity levels of an IFTS and a generic DS, the central conclusion of this paper, i.e. that an IFTS has at least two orders of magnitude speed advantage for execution of the high spectral resolution survey portions of the NGST DRM will be derived. It will be demonstrated that this central conclusion is not an artifact of an overly optimistic estimate of the efficiency of an IFTS relative to
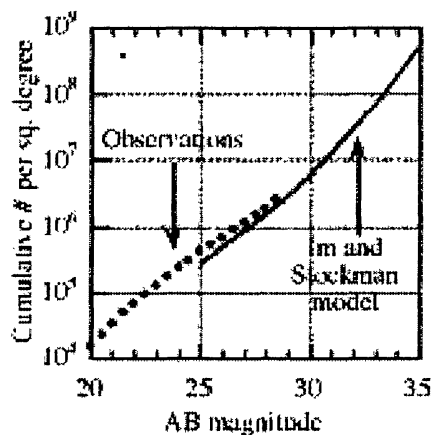
Figure 8.   The observational estimates of K band galaxy cumulative number density vs. limiting magnitude are taken from Yan 1998, Bershady 1998, and Thompson 1999. The extrapolation to fainter magnitudes by Im and Stockman includes evolutionary effects. For the brighter magnitudes, the Im and Stockman model does not include some of the objects counted in the observations.

a DS, but rather is attributable to an intrinsic feature of the imaging Fourier transform spectrometer.

3.   Source Counts

For any given sensitivity level, it is crucial to factor in the expected density of objects that can be observed in order to determine if the acquisition of "a spectrum for every pixel" is worthwhile. Figure 8 displays the observed (Yan, et al. 1998; Thompson, et al. 1999; Bershady, et al. 1998) and extrapolated (Im & Stockman 1998), cumulative number per square degree of galaxies brighter than a given limiting AB magnitude in K band. For the 100 nJy magnitude limit (AB magnitude = 26.4) attainable with an IFTS on NGST in a single day exposure at $R = 5000$, the number of objects per field of view is approximately 5000. The ability to determine redshifts, map large scale structure, measure chemical composition, and measure internal kinematics for all of these objects certainly would provide a very rich source of data. Furthermore, with the IFTS observations, there is always an associated "panchromatic" image obtained, that is sensitive to much fainter levels than would be gotten by simply adding up all of the individual spectral images. The panchromatic image is truly "more than the sum of its parts." In the same 10^5 s observation used to acquire the $R = 3000$ IFTS data-cube, the panchromatic sensitivity level is approximately 0.2 nJy (AB magnitude = 33). At this flux level approximately half a million galaxies are expected per field of view, and it is quite possible that hitherto unknown objects will be observed. The relative performance advantage of an IFTS for achieving

the goals of NGST above all other instrumental architectures would seem to virtually demand that an IFTS be included in the ISIM for NGST.

4.   The SNR for Imaging Spectrometers

The signal to noise ratio, SNR, for either a tunable filter (TF) spectrometer, or a dispersive spectrometer (DS), depends on detector dark current, I_d, read noise, n_r, zodiacal background, $Z(\nu)$, source intensity $S(\nu)$, integration time T_ν, and the effective width of the spectral resolution function, $\Delta\nu_{\text{eff}}$ according to the expression

$$SNR_{\text{TF}} = \frac{\eta \cdot QE(\nu) \cdot S(\nu)\Delta\nu_{\text{eff}}T_\nu}{\sqrt{\{QE(\nu)\cdot(S(\nu)+Z(\nu))\Delta\nu_{\text{eff}}+I_d\}\cdot T_\nu + n_r^2}} \quad . \tag{1}$$

A DS tends to provide spectra that are evenly spaced in wavelength rather than frequency; in this case the substitution of λ for ν is most appropriate. In expression (1), $QE(\nu)$ represents the system efficiency for converting photons incident at the entrance aperture to detected electrons rather than just the quantum efficiency of the detector elements themselves. The efficiency factor encapsulates all effects which lower the signal level without concomitantly lowering the background level, such as surface scattering losses, for example. The effective width of the spectral resolution function is defined for a tunable filter, for example, as the integral of a given filter transmission function over all frequencies divided by the maximum value of the transmission function.

The signal to noise ratio for Fourier transform spectrometers, using the same notation as in expression (1) is given by the expression

$$SNR_{\text{IFTS}} = \frac{\eta \cdot QE(\nu) \cdot S(\nu) \cdot \Delta\nu_{\text{eff}}T_{\text{total}}}{\sqrt{\{\int QE(\nu)\cdot(S(\nu)+Z(\nu))d\nu + 2I_d\}\cdot T_{\text{total}} + 2Nn_r^2}} \quad . \tag{2}$$

Expressions (1) and (2) are derived by Bennett (2000). Very similar expressions are given, without derivation, by Beer (1992). Fourier transform spectrometers have a modulation efficiency factor which enters into the η efficiency factor for the spectrally resolved SNR, but not into the pan-chromatic SNR. The factor of 2 in front of both the detector dark current term and the detector read noise term originates from the use of both output ports of an IFTS. Finally, N is the number of interferogram samples used in computation of the spectra.

For sufficiently long integration times, the detector read noise term may be made negligible, both for the IFTS and the DS. In this limit, and assuming that the efficiency factors η for the DS and IFTS are equal, the ratio of the SNR for the IFTS and the DS is given by

$$\frac{SNR_{\text{IFTS}}}{SNR_{\text{DS}}} = \frac{\sqrt{\{QE(\lambda)\cdot(S(\lambda)+Z(\lambda))\Delta\lambda_{\text{eff}}+I_d\}\,T_{\text{total}}}}{\sqrt{\{\int QE(\nu)\cdot(S(\nu)+Z(\nu))d\nu + 2I_d\}\cdot T_\lambda}} \quad . \tag{3}$$

For a sufficiently small effective width of the spectral resolution function, the DS always becomes dark current limited. In contrast, the IFTS is independent of the dark current (for any of the values being considered for NGST), at all spectral

resolutions. As a specific example, for a bandpass of 1–5 μm, which is easily obtained by the IFTS, the integrated zodiacal light intensity yields a photocurrent of approximately 2.2 e/s, which is an order of magnitude greater than the dark current levels of the currently available generation of InSb detectors (i.e. 2×0.1 e/s). For the faintest sources, i.e. those whose intensity is only a fraction of the Zodiacal background level, the integral over the IFTS bandpass may be well approximated by the value for the Zodiacal background alone. This limit is particularly relevant for emission line sources. In the high resolution limit, and for appropriately faint sources, and using the current generation InSb dark current levels, the SNR ratio between IFTS and DS becomes

$$\frac{SNR_{\mathrm{IFTS}}}{SNR_{\mathrm{DS}}} \approx \frac{\sqrt{0.1(\mathrm{e/s}) \cdot T_{\mathrm{total}}}}{\sqrt{2.4(\mathrm{e/s}) \cdot T_\lambda}} \quad . \tag{4}$$

In this limit, although the DS may attain a higher SNR for a single object, as soon as more than 24 grating settings, or slit mask settings, are required, the IFTS breaks even in sensitivity. If in addition, the overhead involved in deciding which sample of objects is to be observed is properly included, the break even point occurs much more quickly. Furthermore, with prior object selection, an inevitable selection bias is introduced, and the probability of finding the unusual or the unexpected is decreased.

If the DS is used to map the same field of view as the IFTS, as discussed in section 2 above, then the resulting SNR ratio becomes

$$\frac{SNR_{\mathrm{IFTS}}}{SNR_{\mathrm{DS}}} \approx 0.4 \cdot \sqrt{R} \quad . \tag{5}$$

At a spectral resolution of $R \sim 5000$, the IFTS is nearly three orders of magnitude faster than the mapping dispersive spectrometer.

5. Conclusion

In view of the enormous sensitivity advantage of the IFTS relative to all of the other design concepts that have been studied for NGST, it would seem that the original IFTS concept (Graham, et al. 1998), having no dispersive elements, no bandpass defining filters, and no object plane micro-shutter array, provides the optimal match to the core mission of NGST for both imaging and high resolution spectroscopy.

References

Beer, R., 1992, *Remote Sensing by Fourier Transform Spectrometry*, J. Wiley & Sons, New York, p. 62

Bennett, C. L., 2000, in *Imaging the Universe in Three Dimensions: Astrophysics with Advanced Multi-Wavelength Imaging Devices*, ASP Conference Series, eds. W. van Breugel and J. Bland-Hawthorn

Bershady, M., et al. 1998, ApJ, 505, 50

Graham, J. R., Abrams, M., Bennett, C. L., Carr, J., Cook, K., Dey, A., Najita, J., & Wishnow, E. 1998, PASP, 110, 1205

Im, M. & Stockman, H. S. 1998, in *Science with NGST*, eds. E. P. Smith and A. Koratkar, ASP Conf. Ser. Vol. 133, p. 263

Lilly, S. 1999, "NGST integral field spectroscopy at high spectral and spatial resolution,"
http://www.ngst.nasa.gov/cgi-bin/doc?Id=531/

Thompson, R., et al. 1999, ApJ, 117, 17

Yan, L., et al. 1998, ApJ, 503, L19

Charles Bennett

Part 4. September 16: Supporting Technologies